biophysica

MDPI

*Article*

# Evidence of the Differences Between Human and Bovine Serum Albumin Through the Interaction with Coumarin-343: Experimental (ICD) and Theoretical Studies (DFT and Molecular Docking)

**Carmen Regina de Souza [1,*], Maurício Ikeda Yoguim [1], Nathalia Mariana Pavan [1], Nelson Henrique Morgon [2], Valdecir Farias Ximenes [1] and Aguinaldo Robinson de Souza [1]**

[1] Faculty of Sciences, São Paulo State University (UNESP), Bauru 17033-360, São Paulo, Brazil; mauricio.yoguim@unesp.br (M.I.Y.); nathalia.pavan@unesp.br (N.M.P.); valdecir.ximenes@unesp.br (V.F.X.); aguinaldo.robinson@unesp.br (A.R.d.S.)

[2] Institute of Chemistry, University of Campinas (UNICAMP), Campinas 13083-970, São Paulo, Brazil; nhmorgon@unicamp.br

* Correspondence: carmen.souza@unesp.br

**Abstract**

Coumarins are known for interacting with proteins and exhibiting diverse biological activities. This study investigates the interaction between coumarin-343 (C343) and human (HSA) and bovine (BSA) serum albumins. Fluorescence spectroscopy and theoretical simulations, including density functional theory (DFT) and molecular docking, were used to analyze the ligand–protein complex formation. The fluorescence quenching data revealed that C343 binds to both proteins, with binding constants of $2.1 \times 10^5$ mol·L$^{-1}$ (HSA) and $6.5 \times 10^5$ mol·L$^{-1}$ (BSA), following a 1:1 stoichiometry. Binding site markers identified drug site I (DS1), located in subdomain IIA, as the preferential binding region for both proteins. Computational results supported these findings, showing high affinity for DS1, with binding energies of $-69.02$ kcal·mol$^{-1}$ (HSA) and $-67.22$ kcal·mol$^{-1}$ (BSA). While complex formation was confirmed for both proteins, differences emerged in the induced circular dichroism (ICD) signals. HSA displayed a distinct ICD profile compared to BSA in both intensity and absorption maximum. Molecular Docking revealed that the C343 conformation differed between HSA and BSA, explaining the variation in ICD signals. These results highlight the importance of protein structure in modulating ligand interactions and spectral responses.

**Keywords:** coumarin-343; HSA; BSA; molecular docking; DFT; fluorescence; ICD



Academic Editor: Serge Perez

Received: 3 June 2025
Revised: 23 June 2025
Accepted: 9 July 2025
Published: 15 July 2025

**Citation:** de Souza, C.R.; Yoguim, M.I.; Pavan, N.M.; Morgon, N.H.; Ximenes, V.F.; de Souza, A.R. Evidence of the Differences Between Human and Bovine Serum Albumin Through the Interaction with Coumarin-343: Experimental (ICD) and Theoretical Studies (DFT and Molecular Docking). *Biophysica* **2025**, *5*, 27. https://doi.org/10.3390/biophysica5030027



## 1. Introduction

The interaction between biological macromolecules, such as proteins and DNA, with drugs and/or bioactive molecules is a highly relevant area of research in the life sciences [1,2]. This field is grounded in interdisciplinary approaches that integrate chemical, physical, and biological knowledge in order to understand how intermolecular interactions—such as hydrogen bonding, van der Waals forces, and hydrophobic and electrostatic interactions—modulate the structure and function of complex biological systems [3,4].

Among the proteins of pharmacological interest, human serum albumin (HSA) stands out as the most abundant plasma protein in the human body, accounting for approximately

60% of total plasma proteins [5]. HSA is responsible for the transport of a wide variety of endogenous and exogenous compounds, such as hormones, fatty acids, and drugs, directly influencing pharmacokinetic parameters such as bioavailability, half-life, and tissue distribution [6,7]. Structurally, HSA consists of a single polypeptide chain composed of 585 amino acids, organized into three domains (I, II, and III), each subdivided into subdomains A and B (Figure 1) [8]. It possesses three major binding sites (I, II, and III), with site I (DS1) being the most studied due to its high affinity for bulky and hydrophobic ligands [9–12].

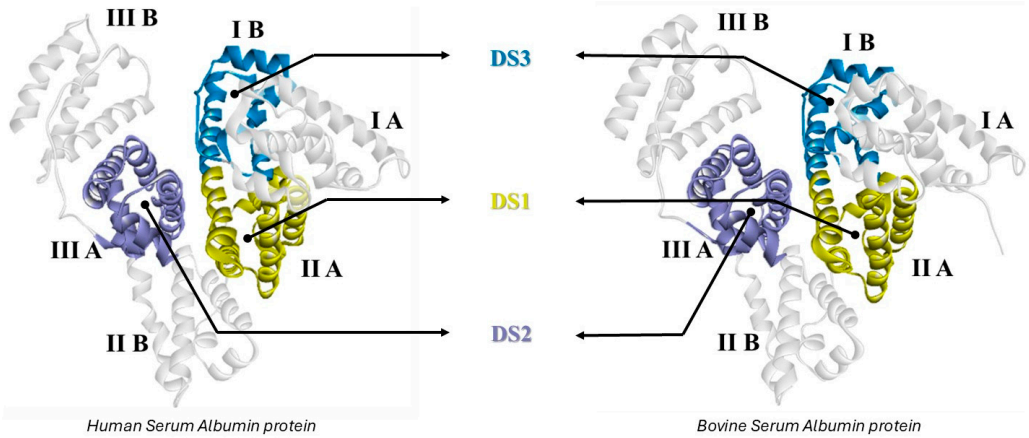


**Figure 1.** Representation of albumin proteins indicating the location of domains, subdomains, and interaction sites: human serum albumin protein—HSA (PDB ID 1AO6) and bovine serum albumin protein—BSA (PDB ID 4F5S).

Similarly, bovine serum albumin (BSA) is widely used as an experimental model in protein–ligand interaction studies due to its high similarity to HSA, showing approximately 80% sequence homology and 76% structural similarity [13–15]. BSA is composed of 582 amino acids and contains two tryptophan residues (Trp-134 and Trp-212), whose intrinsic fluorescence can be quenched in the presence of ligands, enabling the spectroscopic analysis of non-covalent interactions [16–18]. Although the structure of BSA closely resembles that of HSA, differences in amino acid composition and the geometry of the binding sites can result in significant variations in affinity for specific compounds [19–23].

Among bioactive ligands, coumarins are a class of natural and synthetic compounds widely studied in pharmacological and biomolecular research due to their diverse biological activities. Naturally characterized as 1,2-benzopyrones (Figure 2a), they are broadly distributed in plants, fungi, and bacteria. Advances in synthetic chemistry have expanded the chemical diversity of coumarins, facilitating their structural modification and discovery across a wide range of compounds. Their ability to engage in non-covalent interactions with various enzymes and receptors in living organisms gives rise to a broad spectrum of biological applications [24,25].

Among these, coumarin-343 (C343, Figure 2b) stands out as a fluorescent probe widely used in biochemistry and molecular biology research. Its rigid molecular structure, intense fluorescent emission, and remarkable photophysical properties—such as fluorescence and solvatochromism—make it especially suitable for investigating protein–ligand interactions [26,27]. Notably, C343 is frequently employed to study the interaction between coumarin derivatives and albumin proteins, particularly human serum albumin (HSA) and bovine serum albumin (BSA), offering valuable insights into binding mechanisms and molecular recognition processes [24,28,29].

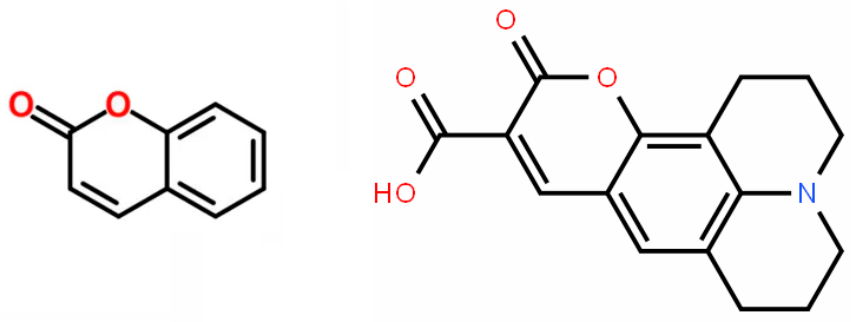


(**a**) (**b**)

**Figure 2.** Molecular structure of (**a**) 1,2-benzopyrone and (**b**) coumarin-343 (C343).

Given the relevance of these interactions in the biomolecular, pharmacological, and biophysical contexts, the aim of this study is to investigate, through a theoretical and experimental approach, the formation of a complex between coumarin-343 and the proteins HSA and BSA. To this end, the binding constant (Ka) was determined through the quenching of the intrinsic fluorescence of the proteins, and binding stoichiometry was assessed using the Job plot method. Furthermore, the preferred binding site of coumarin on HSA was identified based on spectral shifts and molecular docking simulations, and the thermodynamic parameters of the interaction were estimated from experiments conducted at different temperatures.

Conformational changes in the proteins induced by coumarin binding were examined using induced circular dichroism (ICD) spectroscopy, with data subsequently correlated with density functional theory (DFT) calculations to elucidate the electronic effects of the interaction. Finally, the predominant interactions between coumarin-343 and the amino acid residues at the albumin-binding sites were confirmed based on theoretical docking results, integrating experimental and computational data for a comprehensive characterization of the molecular recognition mechanisms.

## 2. Materials and Methods

### *2.1. Materials*

Equipment included a fluorescence spectrometer (Perkin-Elmer LS55, IL, USA) attached to a microprocessor heating system, Control MPC (Huber); an analytical balance (AG245—Mettler Toledo, Switzerland); pH meter (300 Digital–Analyzer); a UV-Vis spectrophotometer (Agilent Technologies Cary 8454); an electronic circular dichroism—ECD (Jasco J-815 CD spectrometer); and a solution agitator (tube agitator MA 162 Marconi). Software included Genetic Optimization for Ligand Docking 2024.2.0 (GOLD), Discovery Studio Visualizer 2021 (DS), Origin Pro 8 2024, GraphPad Prism 7-7, Gaussian 16, Gaussian09, GaussView 6-6.1.1, and GraphPad Prism 5 (version 7.04, GraphPad Software, Inc., San Diego, CA, USA). The solutions used were HSA (A3782) 1.0 mmol·L$^{-1}$ in 50 mmol·L$^{-1}$ phosphate buffer pH 7.0 and C343 (10.0 mmol·L$^{-1}$) in dimethyl sulfoxide. To prepare the BSA solution, 0.033 g of BSA (7030 TRIS) was weighed and dissolved in 0.5 mL of buffer solution, obtaining a final concentration of 1.0 mmol·L$^{-1}$. Warfarin (10 mM) was dissolved in ethyl alcohol. The proteins and chemicals were obtained from Sigma-Aldrich.

### *2.2. Methods*

#### 2.2.1. Binding of C343 and Proteins

Protein solutions at concentrations of 10.0 µmol·L$^{-1}$ (2.0 mL) were added to a 2.0 mL quartz cuvette with a 10.0 mm optical path. The solutions were put through the fluorescence equipment to determine the protein spectrum, with excitation of 295 nm and

emission recorded in the 310–450 nm range. After determining the protein's fluorescence spectrum, aliquots of 0.5 µL of C343 (10.0 mmol·L$^{-1}$) were added, each aliquot accounting for 2.5 µmol·L$^{-1}$ in the resulting solution. The additions were performed in succession until the C343 solution reached a final concentration of 20.0 µmol·L$^{-1}$. The spectra were recorded after 2 min of incubation.

#### 2.2.2. C343 and Albumin Protein Stoichiometry

The stoichiometry of the interaction was determined by the Job plot method. Ten solutions containing C343 and HSA were prepared, each with different concentrations between 1.0 and 10.0 µmol·L$^{-1}$ for each component. The sum of the molarities of the ligand and the protein always equals 11.0 µmol·L$^{-1}$. The fluorescence intensity of each solution was recorded using the following parameters: excitation at 340 nm, emission at 480 nm. A graph was generated with the fluorescence intensity on the *y*-axis and the mole fraction of C343 on the *x*-axis (Equation (1)).

$$X_{C343} = \frac{X_{C343}}{X_{C343} + X_{HSA}} \quad (1)$$

#### 2.2.3. Electronic Circular Dichroism Spectroscopy

CD experiments were performed using a Jasco J-815 spectropolarimeter (Jasco, Japan) equipped with a thermostatically controlled cell holder. The spectra were obtained with 1 nm step resolution, a response time of 1 s, and a scanning speed of 50.0 nm/min. A 3 mL quartz cuvette, magnetically stirred with a 10 mm path length, was used for measurements in the near-UV-CD range. The baseline was a 50.0 mmol·L$^{-1}$ phosphate-buffered solution. Unless otherwise stated, the experiments were performed with HSA and BSA (30.0 µmol·L$^{-1}$) and C343 (10.0 µmol·L$^{-1}$) in 50.0 mmol·L$^{-1}$ phosphate buffer, pH 7.0, at 20 °C.

#### 2.2.4. Molecular Docking Studies

Molecular docking was performed for the DS1 of HSA and BSA. The crystallographic structure chosen for this study was the PDB 2XW0 [12], which contains the dansyl-L-phenylalanine structure at DS1, with a resolution of 2.40 Å, for HSA. The crystallographic structure used in studies with the BSA protein was PDB 4OR0 with a resolution of 2.58 A, and this structure is complexed with naproxen at the DS1, DS2, and fatty acid 6 (FA6) sites [30]. The crystallographic structures were analyzed on the DS and Chimera 1.7.1 software to ensure the existence of some kind of similarity between them so that the docking results would be comparable. The structure of C343 was constructed in the GaussView 6 software and then analyzed on the Discovery Studio Visualizer 2021 (DS) software to determine if the input reading was correct so that the molecular docking studies could go forward.

The molecular redocking and docking studies were performed in the GOLD 2022.3.0 software, using *chemscore_kinase* as the calculation parameter, with a GoldScore scoring function based on Equation (2). Here, S (hb_ext) represents the energy of the ligand protein's hydrogen bond (HB); S (vdw_ext) is the energy of protein–ligand interactions of the van der Waals type, and S (int) corresponds to a penalty for not taking in the internal interactions of the ligand [31,32].

$$Fit\ function = S\ (hb\_ext) + 1.3750 \times S\ (vdw\_ext) + S\ (int) \quad (2)$$

Besides determining the conditions of the function parameters, it is also possible to vary the study radius of the ligand as well as, when feasible, alter the conditions of the amino acids (protonated, rotation, or loose) present in the side chains. Ten analyses were conducted for each of the studies. The analysis of the results obtained by both

molecular redocking and docking was carried out in the DS software. Initially, using this software, visual analyses regarding the positions of the conformations obtained through the calculations were performed to correlate them to their energetic values. Subsequently, the interactions between the probe and the protein's amino acids in the studied sites were assessed in the same software.

## 3. Results

### *3.1. Binding of C343 in HSA and BSA*

Studies to assess the affinities of C343 to HSA and BSA involved the analysis of fluorescence spectra under specific conditions, both in the presence and absence of the ligand, with a protein concentration of 10.0 μmol·L$^{-1}$. Figure 3 shows that when C343 is present, there is progressive decay in the fluorescence intensity with the increase in coumarin in the solution of HSA and BSA. As this process represents an equilibrium state of free and bound C343, adding the ligand decreases the free proteins, resulting in a decrease in the fluorescence intensity.

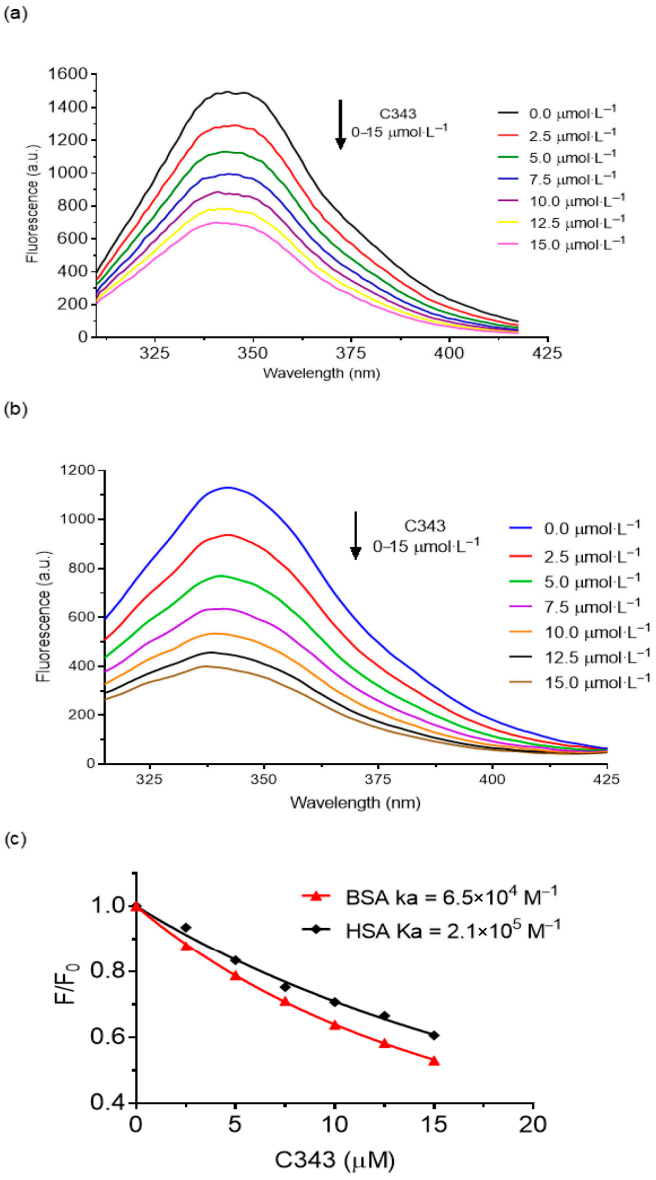


**Figure 3.** (**a**) Fluorescence quenching of BSA due to adding C343; (**b**) fluorescence quenching of HSA due to the addition of C343; (**c**) Ka of C343 with HSA and BSA.

Tryptophan, tyrosine, and phenylalanine are responsible for the fluorescence emission of proteins when excited at around 280 nm. However, phenylalanine and tyrosine exhibit low quantum efficiency at this wavelength due to ionization processes and the effects of induced polarization in the microenvironment surrounding these amino acids. Consequently, the primary natural fluorophore in proteins is tryptophan, which emits fluorescence at 350 nm [7,33–36].

Figure 3 shows that the maximum value of fluorescence emissions occurs at 342.0 and 345.5 nm for HSA and BSA, respectively. Thus, the amount of protein complexed with the addition of C343 was calculated, which involved subtracting the fluorescence intensity with the presence of the ligand from the free protein (at λ = 342.0 nm and 343.5 nm).

The determination of the association constant (Ka) between bioactive ligands and plasma proteins is a crucial step in understanding the mechanisms of drug transport, distribution, and bioavailability in the human body. Specifically, in the case of human serum albumin (HSA), such interactions directly influence the pharmacokinetics of bioactive compounds, affecting their therapeutic activity and metabolism [16,37].

In this study, the association constant for the complex formed between coumarin-343 (C343) and HSA was determined using spectrofluorimetric measurements. The Ka value was calculated using an equation based on the mathematical models proposed by Hildebrand and Benesi (1949), and later adapted by Lakowicz (2006); Rawel, Meidtner, and Kroll (2005); Roy (2004); and Zsila, Hazai, and Sawyer (2005) [38–42]. These models correlate the fluorescence intensity of the protein–ligand system at varying ligand concentrations, enabling the quantification of complex formation (Equation (3)).

$$\frac{F}{F_0} = 1 - \varphi \frac{\left[ (K_d + P + L) - \sqrt{(K_d + P + L)^2 - 4 \cdot P \cdot L} \right]}{2 \cdot P} \quad (3)$$

From the fluorescence spectra obtained experimentally, it was observed that the maximum emission peak of free HSA occurs at 342 nm (Figure 3). The formation of the C343-HSA complex was monitored through changes in fluorescence intensity at this wavelength, allowing for the calculation of the complexed protein fraction. The observed fluorescence (Fobs) was determined by subtracting the spectra obtained in the presence of the ligand from those of the free protein.

To minimize the optical interference caused by absorbance at excitation and emission wavelengths, the fluorescence values were corrected according to the equation proposed by [43]. This correction considers the system's absorbance at the excitation (Aexc) and emission (Aem) states, resulting in the corrected fluorescence (Fcorr), as defined in Equation (4).

$$F_{corr} = F_{obs} \times 10^{\frac{(Aexc + Aem)}{2}} \quad (4)$$

Subsequently, the corrected values were normalized by subtracting the initial fluorescence and dividing by the corrected fluorescence value. Based on these data, a graph was constructed (Figure 4), from which a linear regression was performed to obtain the intercept and slope coefficients. These coefficients were applied to Equation (1) to determine the association constant, Ka.

The calculated association constant for the C343-HSA complex was $2.10 \times 10^5$ mol·L$^{-1}$, a value consistent with typical constants reported for similar ligand–protein systems, which commonly fall within the range of $10^4$ to $10^6$ mol·L$^{-1}$, confirming the coherence and plausibility of the value obtained for C343 in this study. The association constant for the C343-BSA complex was $6.50 \times 10^4$ mol·L$^{-1}$. The lower affinity of C343 with BSA agrees with the values reported by Datta and Halder, who demonstrated inherent structural and functional deviations between HSA and BSA, leading to a significant difference in behavior

toward C343 at DS1 [23]. We propose that this feature is responsible for the difference in the induction of chirality in C343, as will be shown in the next sections.

### *3.2. Stern–Volmer*

Static and dynamic quenching can be determined by the relationship between the values of the binding constants and the temperature. In static quenching, the values of the binding constants decrease while the temperature increases due to the complex's drop in stability as the temperature rises. In dynamic quenching, the opposite happens. The binding constants increase with the temperature due to the rise in collisions as the temperature rises [44].

Table 1 details the values, in triplicate, for the determination of the Ksv of HSA with C343 at different temperatures. Due to the similarity between the proteins, the same parameters and results were adopted for BSA.

**Table 1.** $K_{SV}$ at different temperatures.

| Temperature (K) | $K_{SV}$ ($mol^{-1} \cdot L$) | Kq ($mol^{-1} \cdot L \cdot s^{-1}$) | $R^2$ |
|---|---|---|---|
| 293 | $3.09 \times 10^5$ | $3.09 \times 10^{13}$ | 0.9903 |
| | $3.01 \times 10^5$ | $3.01 \times 10^{13}$ | 0.9925 |
| | $3.05 \times 10^5$ | $3.05 \times 10^{13}$ | 0.9926 |
| 313 | $1.57 \times 10^5$ | $1.57 \times 10^{13}$ | 0.9979 |
| | $1.52 \times 10^5$ | $1.52 \times 10^{13}$ | 0.9986 |
| | $1.37 \times 10^5$ | $1.37 \times 10^{13}$ | 0.9994 |

Therefore, the experimental results suggest that, by increasing the temperature, there is a decrease in the Stern–Volmer constant ($K_{sv}$) value, thus indicating static quenching with complex formation in its fundamental state.

However, the bimolecular suppression constant value (Kq) stays above $10^{10}$ $mol^{-1} \cdot L \cdot s^{-1}$, suggesting static quenching. The average square deviation value ($R^2$) staying near 1 illustrates that there is predominantly only one type of quenching.

### *3.3. Determination of Stoichiometry*

The accurate determination of the stoichiometry of protein–ligand interactions is fundamental for understanding how bioactive molecules behave in physiological environments. In drug design and molecular recognition studies, knowing the binding ratio between a ligand and its protein target allows researchers to predict biological activity, optimize dosing strategies, and refine molecular modeling. In this context, coumarin-343 (C343), a fluorescent probe with significant biological and pharmacological relevance, was studied for its interaction with human serum albumin (HSA), a key plasma transport protein.

Considering the widespread use of albumin-binding ligands in therapeutic and diagnostic applications, defining the binding stoichiometry becomes essential. A 1:1 ratio, for instance, may suggest a single dominant interaction site, whereas more complex ratios might indicate cooperative or multi-site binding, which could impact bioavailability and efficacy. Given these implications, the present study employed Job's method of continuous variation to quantitatively assess the interaction between C343 and HSA.

Job's method is particularly suited for this purpose, as it allows for the determination of complex stoichiometry through experimental measurements that monitor molecular interaction, in this case, fluorescence intensity. To apply the method, a series of ten mixtures were prepared in which the molar ratio of C343 to HSA varied systematically while keeping

the total concentration constant at 11 μmol·L$^{-1}$. Fluorescence spectroscopy was used to monitor the formation of the protein–ligand complex across different compositions.

The resulting data were plotted as fluorescence intensity versus the molar fraction of C343 (Figure 4). Two linear regressions—applied to the ascending and descending regions of the curve—intersected at a molar fraction of 0.44. This point of intersection indicates the maximum extent of complex formation and reveals the optimal stoichiometric ratio between the two interacting species [45,46].

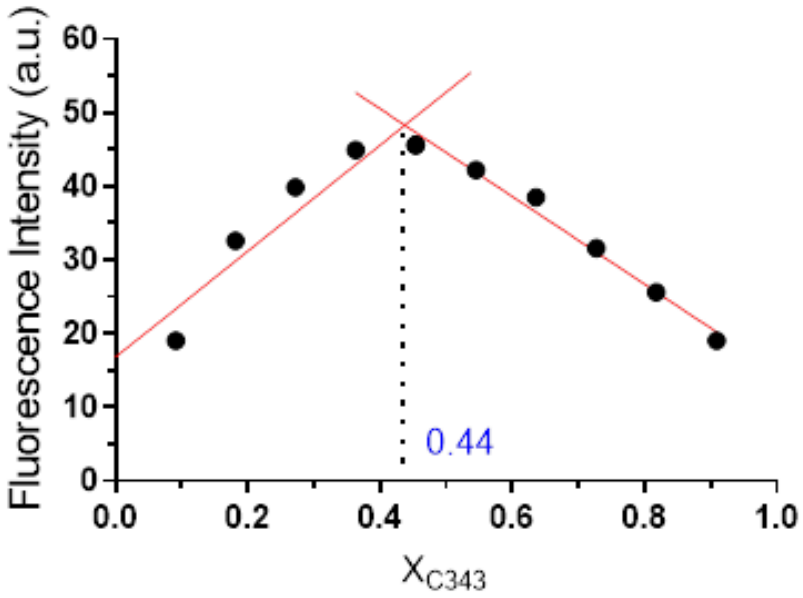


**Figure 4.** Job's method graph.

Further analysis using the molar fraction equation demonstrated that 0.616 mol·L$^{-1}$ of HSA binds with 0.484 mol·L$^{-1}$ of C343, resulting in a stoichiometric ratio of approximately 1:1.12. This near-equimolar interaction supports the notion of a dominant, specific binding event between C343 and a single site on the HSA protein.

Based on this established stoichiometry, the study proceeded with site identification through competitive binding assays, using well-characterized drugs to probe the canonical binding sites of HSA. These experiments aimed to confirm not only the binding ratio but also the preferential localization of the C343 molecule within the protein's structure.

In conclusion, the use of Job's plot methodology provided both quantitative and mechanistic insights into the interaction between C343 and HSA. The identification of a ~1:1 binding ratio reinforces the hypothesis of selective and specific recognition, forming the basis for deeper molecular-level investigations and future pharmacological exploration

### *3.4. Determination of Preferential Binding Sites*

Identifying the preferred binding site of a ligand on a protein target is a fundamental step in elucidating the mechanisms of molecular recognition and guiding the rational design of bioactive compounds. In this study, we employed a site-competition fluorescence assay to determine the primary binding region of coumarin-343 (C343) on human serum albumin (HSA), a key plasma protein involved in drug transport.

The experimental design began with the formation of the C343-HSA complex in solution under controlled conditions, ensuring that the system was at equilibrium. Following this, incremental additions of the site-specific markers to the solution were performed. The central hypothesis is that if a marker binds to the same site as C343, it will compete with the fluorophore, leading to detectable changes in the fluorescence emission spectrum of

the system. In contrast, if the marker binds to a different site, no significant change in the fluorescence pattern is expected.

This logic is schematically illustrated in Figure 5. Initially, the free HSA interacts with free C343 to form a stable protein–ligand complex. Upon the addition of a site-specific competitor, two distinct outcomes are possible. In Pathway I, the marker displaces or interferes with C343 at the same binding site, resulting in fluorescence quenching or spectral shifts—clear indicators of competitive binding. In Pathway II, however, the marker binds at an alternative site, leaving the C343-HSA complex unaffected, and thus the fluorescence profile remains unchanged.

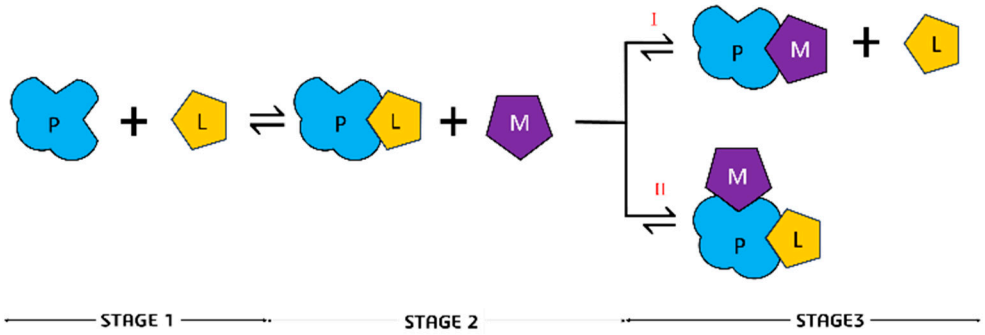


**Figure 5.** Site competition mechanism with its possible paths, with P = protein, L = ligand, and M = marker.

By comparing the spectral behavior of C343 in the presence and absence of each site marker, one can infer the site-specific affinity of the ligand. This approach provides a non-invasive, spectroscopic route to localize ligand binding, complementing molecular docking and thermodynamic analyses. Furthermore, the use of intrinsic fluorescence of C343 enhances the sensitivity of the method, allowing subtle changes in interaction dynamics to be detected with high resolution.

Ultimately, this competitive displacement strategy contributes critical insight into the molecular determinants of C343 binding, clarifying whether its interaction with HSA is localized to a canonical drug-binding pocket or involves an alternative site. Such information is not only valuable for interpreting in vitro results but also for predicting in vivo pharmacokinetic behavior of coumarin-derived compounds.

The fluorescence results of the site competition studies are represented in Figure 6.

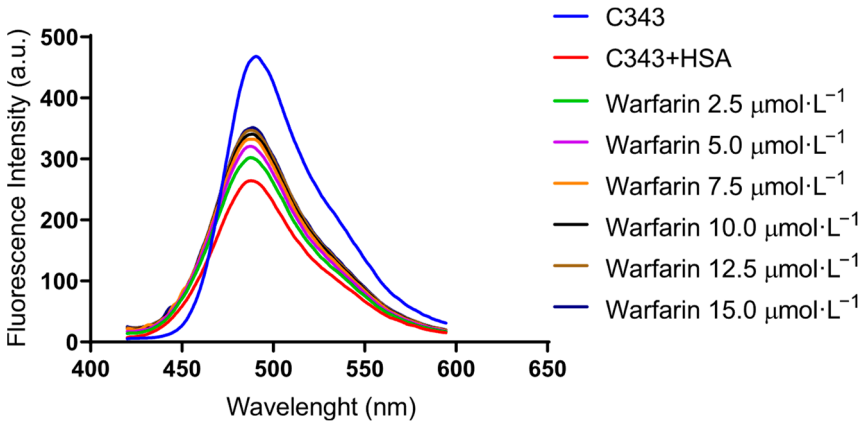


**Figure 6.** Displacement of C343 from HSA; effects of adding warfarin on the fluorescence spectrum of C343 + HSA.

Figure 6 shows that when warfarin was added at a 2.5 μmol·L$^{-1}$ (green-colored), the fluorescence spectrum shows a hyperchromic increase compared to C343 + HSA. This indicates that warfarin decreases the concentration of the C343 + HSA complex, increasing the amount of free C343. As such, it can be attested that there is competition between C343 and warfarin in interacting with site DS1 of the HSA protein. It can also be observed that by adding an increasing amount of warfarin, the hyperchromic increase reaches a maximum, indicating that not every C343 complex is transformed into free C343. Furthermore, even when the warfarin concentration is higher than that of C343, it cannot completely transform the complex ligand to the free form, evidencing the higher affinity of C343 at DS1. These results demonstrate the higher affinity of C343 to the DS1 site of HSA, located at the IIA subdomain.

### *3.5. Molecular Docking Results*

Molecular docking plays a fundamental role in predicting the sites of highest affinity, enabling a detailed analysis of molecular interactions and contributing to the understanding of the mechanisms of molecular recognition of C343 in HSA.

To ensure the efficiency of the study, the crystallographic structure selected was PDB 2XW0 [12], which contains dansyl-L-phenylalanine in the DS1 and DS2 sites and presents a resolution of 2.40 Å.

The redocking and molecular docking studies were performed in the GOLD 2022.3.0 software, using the chemscore_kinase scoring parameter with the Goldscore scoring function, described by Equation (2).

Here, S (hb_ext) represents the energy of hydrogen bonds between the protein and the ligand, S (vdw_ext) corresponds to the energy of van der Waals interactions, and S (int) is a penalty for internal adjustments of the ligand [31,32].

Molecular docking also allowed for variation in the ligand's study radius and, when necessary, adjustments to the protein's amino acids, including protonation, rotation, and flexibilization of the side chains. For each calculation, ten separate analyses were conducted, ensuring a robust set of data for interpretation.

The results were evaluated using the DS software, initially through a visual inspection of the generated conformers, correlating their positions with the energy values obtained. Then, the specific interactions between C343 and the amino acid residues at the studied site were analyzed.

The importance of molecular docking in this study lies in its ability to predict molecular interactions with a high level of detail, allowing not only for the identification of preferred binding sites but also the understanding of the stability and interaction patterns of C343 with HSA. These results are important for the development of new biotechnological and pharmacological applications, aiding in the rational design of drugs and biomarkers.

Even though the proteins are homologous, some amino acids involved in this region are different, and consequently, the numbering of similar amino acids is distinct, as demonstrated in the amino acid sequence illustrated in Figure 7.

Molecular docking studies at the DS1 site were performed with a radius of 7 Å and the flexibilization of the amino acid. Arginine-218 of the side chain yielded an energy value of −69.02 kcal·mol$^{-1}$ for this site.

The interactions of BSA with coumarin-343 at the DS1 site are of the hydrogen-bonding type with the amino acids arginine-194 (1.63 Å, 1.97 Å, and 2.94 Å), arginine-198 (2.24 Å), arginine-217 (2.52 Å), serine-201 (2.22 Å), leucine-197 (2.77 Å), and tryptophan-213 (2.19 Å), the latter being of the π-donor type. There are hydrophobic interactions with the amino acids leucine-197 (4.02 Å) and valine-342 (4.68 Å), and three interactions occurring with the amino acid tryptophan-213 (3.99 Å, 4.19 Å, and 4.35 Å).

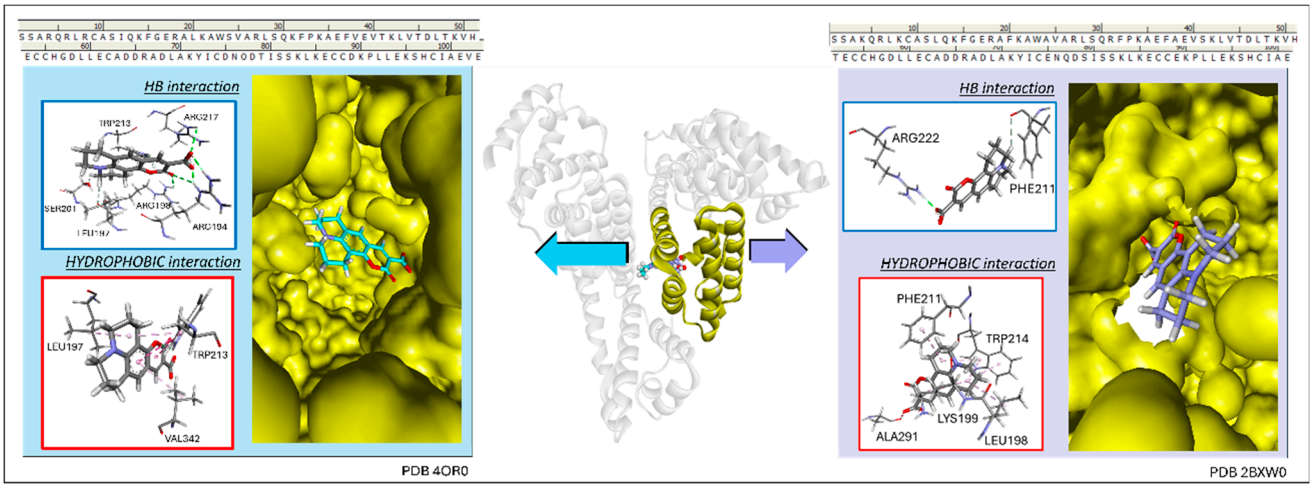


**Figure 7.** Hydrogen bonding and hydrophobic interactions between C343 and site 1 of HSA (purple) and BSA (blue).

### *3.6. Density Functional Theory Calculations*

DFT calculations were performed on the GridUnesp servers. The functionals used were B3LYP and CAM-B3LYP. The B3LYP functional, called Becke's three-parameter exchange functional (B3LYP), is an empirical combination of Hartree–Fock and DFT exchange functionals, associated with the Lee–Yang–Parr (LYP) correlation functional, developed by Lee, Yang, and Parr. The correlation between these functionals resulted in the hybrid functional B3LYP [37].

The basis set used in this study was ***6-311++G(2d,p)***, where the notation ***6-311*** represents six primitive Gaussian functions and three sets of Gaussian functions. The **++** notation indicates that the first **+** adds diffuse functions to heavy elements, while the second **+** adds diffuse functions to hydrogen atoms. The ***2d,p*** notation represents polarization, where ***2d*** corresponds to two sets of polarized ***d***-type functions added to the heavy atom, and ***p*** corresponds to ***p***-type polarization added to the hydrogen atom. The Cartesian coordinates of C343 used in this study were based on the structure obtained from molecular docking calculations [47,48].

Studies also considered variations in the microenvironment, including the addition of implicit and explicit solvents, in addition to performing calculations in vacuum. The solvents were water, dimethyl sulfoxide (DMSO), acetonitrile, and ethanol. However, the best results of the ICD spectra were observed in conditions without the added solvents. Furthermore, studies were carried out with dihedral variations in C343, covering a scan from 30° to 360°, with 30° increments. Thus, a total of 12 conformations were obtained for each dihedral angle, which were subsequently optimized using the same theoretical level used in the scan. The results obtained from these analyses allowed for the determination of the theoretical ICD.

### *3.7. Induced Circular Dichroism Experiments*

In circular dichroism, chiral center and their enantiomers are visualized based on the deviation of circularly polarized light. When a ligand complexes with a protein, it may present a chiral center induced by the protein environment, even if it does not have chiral atoms in its free form [26,49,50]. C343 does not have an isolated ECD signal, indicating the absence of chirality as expected, since it is not an optically active molecule, and there are no chiral carbons in its structure. Analyzing Figure 8, we observe the appearance of an ICD signal indicative of the presence of C343 and HSA, a negative band at 419 nm, and

a positive band at 466 nm, thus indicating that C343 acquires chirality when interacting with HSA.

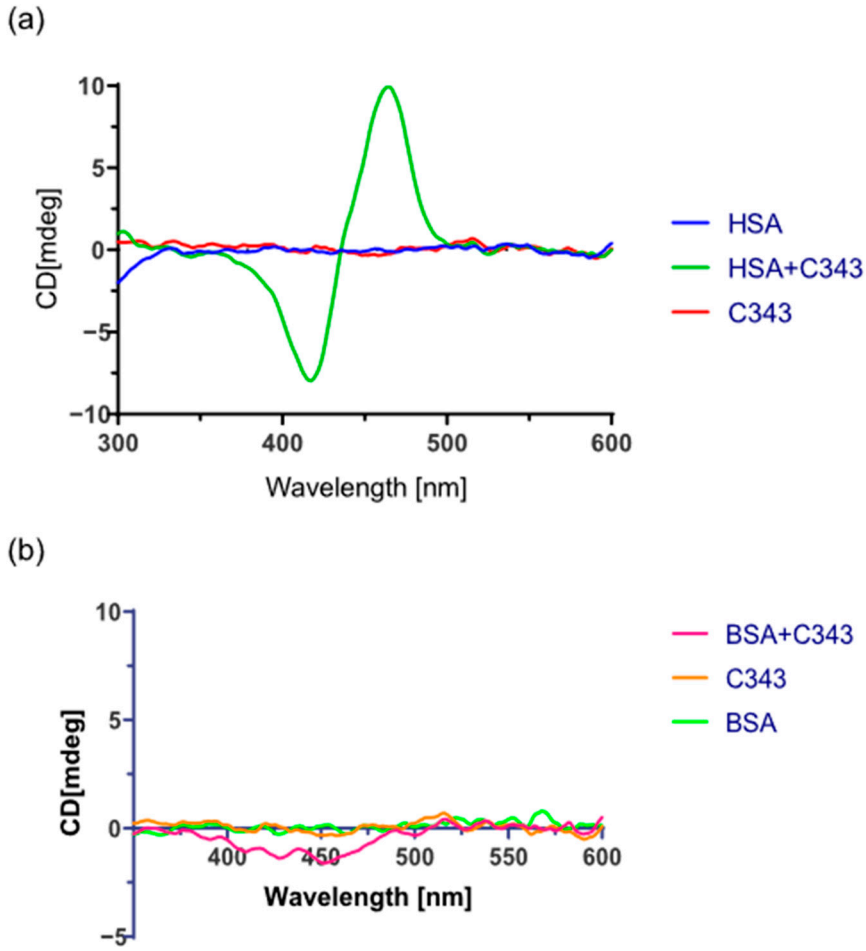


**Figure 8.** ICD spectra of free C343, free protein: (**a**) C343 + HSA and (**b**) C343 + BSA.

In the computational simulation of ICD, we obtained results like the experimental ones, where there is a signal for the interaction of C343 with HSA and a much less intense signal in BSA. To obtain these theoretical results of ICD, it was necessary to obtain a more favorable environment, close to the experimental one. Thus, in the computational model, the amino acid arginine-218 was inserted in the calculations for HSA and arginine-194 for BSA. Due to the greater interaction with DS1, the calculations were performed based on the coordinates of the conformer obtained in the molecular docking studies for this site, both for HSA and BSA.

Analyzing Figure 9, it is possible to observe that the theoretical ICD spectra obtained resemble the experimental ones, reaffirming that the structure obtained from docking is one of the possible conformers that C343 has in the formation of the complex in DS1 of HSA and BSA. From the conformers obtained in docking and the study of the carbonyl dihedra of each of them, it was possible to obtain the most likely conformer that complexed with the proteins under study.

The conformers obtained for each of the proteins have dihedrals, in relation to the carbonyl group and the protein, of 300° and 270° for HSA and BSA, respectively. A similar study for the two conformers was performed, and in Figure 10, we present the calculated RMSD value equal to 0.35; this difference, mainly in the carboxyl group, suggests the discrepancy between the ICD spectra of HSA and BSA in the presence of different amino acids.

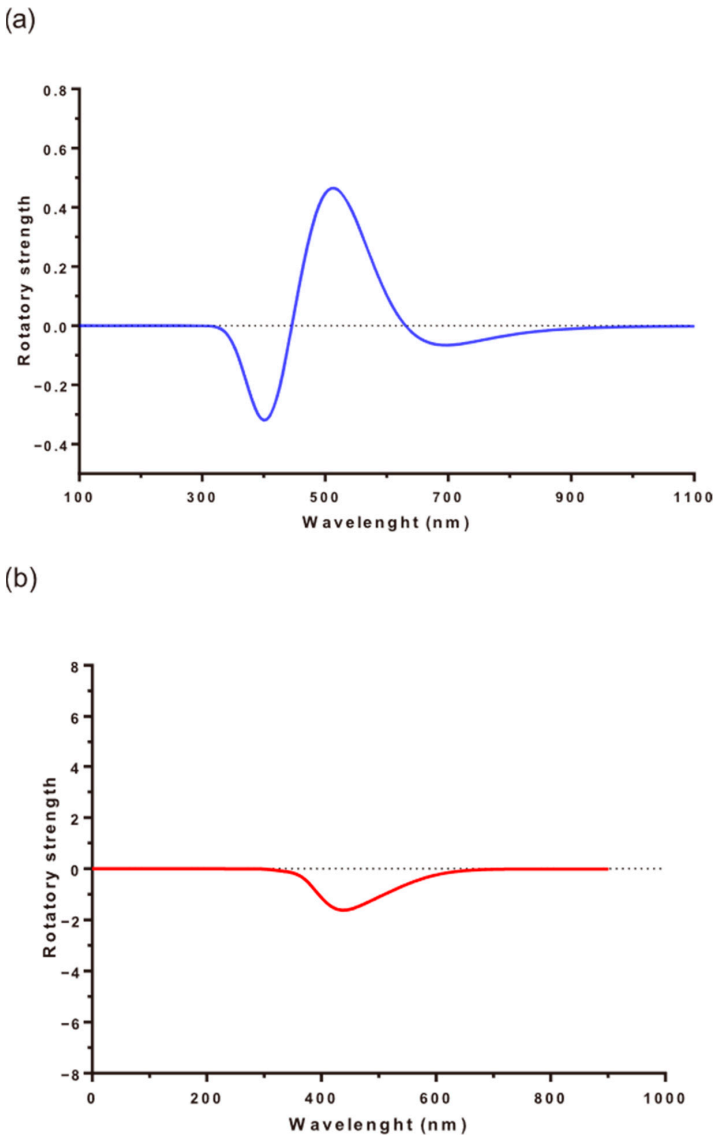


**Figure 9.** Theoretical ICD of (**a**) C343 + HSA and (**b**) C343 + BSA.

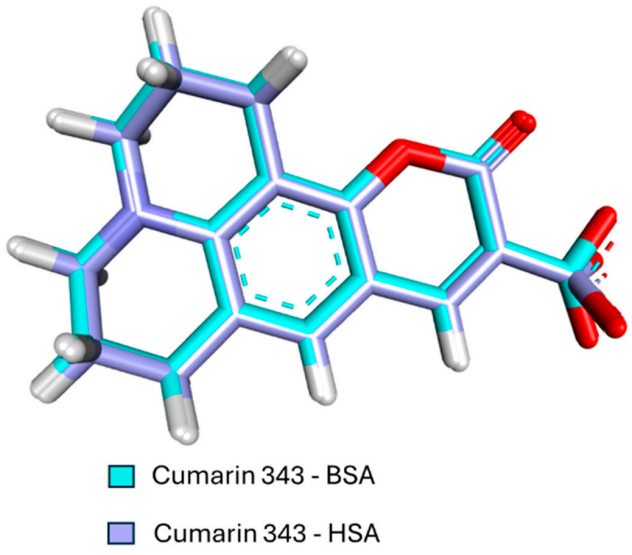


**Figure 10.** RMSD of C343 conformers in HSA and BSA.

## 4. Conclusions

In the analysis of the interaction of C343 with the proteins, the values of the association constants, Ka, were obtained for the proteins HSA and BSA, where the complexation of C343 with the two proteins was verified. The values differed by about 10 times in relation to HSA and BSA, indicating that C343 complexes more strongly with HSA compared to BSA. The association constant in HSA is $2.1 \times 10^5$ Mol·L$^{-1}$, while in BSA it is $6.5 \times 10^4$ mol·L$^{-1}$.

Through site competition experiments with the warfarin molecule, the DS1 site was the preferred binding site of C343 for HSA. We found that the same phenomenon occurred for BSA, as evidenced by the homology between the two proteins. In the search for protein–ligand stoichiometry, we used the Job plot method, where the value obtained was in the proportion of 1:1 of C343 and HSA.

In the molecular docking study, it was possible to observe the possible interactions of the C343 molecule in the DS1 sites of HSA and BSA. This study also allowed us to obtain the two conformers used for the DFT study in the ICD calculation.

This study revealed that HSA and BSA proteins, despite having high compositional and structural similarity, presented different behaviors regarding the interaction with the C343 molecule. Molecular docking studies clearly demonstrated that the bonds between C343 in the DS1 site of HSA were different from those of BSA. Further studies should be performed to better understand this behavior, such as confirming the DS1 site as preferential for BSA and the competition of sites with other molecules, in addition to warfarin. The ICD spectra clearly showed that the conformational structure adopted by C343 in the DS1 site of HSA was different from that adopted in BSA. The adoption of BSA as a model for HSA should be reviewed, since in the interactions with the C343 molecule, we observed a significant difference in relation to the phenomenon of formation of molecular complexes, an area of great relevance in the study of interactions between drugs and proteins.

**Author Contributions:** Conceptualization and methodology, C.R.d.S., M.I.Y., N.M.P., N.H.M., V.F.X. and A.R.d.S.; data curation, C.R.d.S., N.H.M., V.F.X. and A.R.d.S.; writing, C.R.d.S. All authors have read and agreed to the published version of the manuscript.

**Funding:** This research was funded by CAPES, CNPQ (N°: 302121/2022-6) and FAPESP (N°: 2013/08293-7, 2015/22338-9, 2018/12950-7, 2019/12294-5, 2019/18445-5, 2020/05535-3, and 2024/00959-0).

**Data Availability Statement:** All data and their source are included in Section 2 and references.

**Acknowledgments:** The authors would like to thank the CAPES, CNPq, and FAPESP for the financial support and resources provided.

**Conflicts of Interest:** The authors declare no conflicts of interest.

## References

1. Guido, R.V.C.; Andricopulo, A.D.; Oliva, G. Planejamento de fármacos, biotecnologia e química medicinal: Aplicações em doenças infecciosas. *Estud. Av.* **2010**, *24*, 81–98. [CrossRef]
2. Yoguim, M.I. *Estudos da Interação da Rosa de Bengala com a Proteína Albumina do Soro Humano (HSA) sob Aspectos Experimentais e Teóricos na Caracterização dos Sítios de Ligação*; Universidade Estadual Paulista "Júlio de Mesquita Filho": Bauru, Brazil, 2021.
3. Lehn, J.-M.; Sanders, J.K.M. Supramolecular chemistry: Concepts and perspectives. *Angew. Chem. Int. Ed. Engl.* **1995**, *34*, 2563. [CrossRef]
4. Pacheco, I.B. *Estudo Molecular e Espectroscópico da Interação de Derivados Dihidropiridínicos com o DNA.*; Universidade Federal de Santa Catarina: Florianópolis, Brazil, 2023.
5. Lindup, W.E.; Orme, M.C. Clinical pharmacology: Plasma protein binding of drugs. *Br. Med. J.* **1981**, *282*, 212–214. [CrossRef] [PubMed]

6. Zhang, D.; Jiang, X.; Yang, H.; Martinez, A.; Feng, M.; Dong, Z.; Gao, G. Acridine-based macrocyclic fluorescent sensors: Self-assembly behavior characterized by crystal structures and a tunable bathochromic-shift in emission induced by via adjusting the ring size and rigidity. *Org. Biomol. Chem.* **2013**, *11*, 3375–3381. [CrossRef] [PubMed]
7. Al-Harthi, S.; Lachowicz, J.I.; Nowakowski, M.E.; Jaremko, M.; Jaremko, Ł. Towards the functional high-resolution coordination chemistry of blood plasma human serum albumin. *J. Inorg. Biochem.* **2019**, *198*, 110716. [CrossRef] [PubMed]
8. Srivastava, K.; Singh, S.; Kumar, P.; Kumar, R. Review of post-translational modification of human serum albumin: A potential marker with altered structure and function. *Int. J. Biol. Macromol.* **2020**, *164*, 482–492.
9. Nelson, D.L.; Cox, M.M.; Lehninger, A.L. *Princípios de Bioquímica de Lehninger*, 5th ed.; Artmed: Porto Alegre, Brazil, 2011; p. 1273, ISBN 9788536324180.
10. Carter, D.C.; Ho, J.X. Structure of serum albumin. *Adv. Protein Chem.* **1994**, *45*, 153–203. [CrossRef] [PubMed]
11. Ghuman, J.; Zunszain, P.A.; Petitpas, I.; Bhattacharya, A.A.; Otagiri, M.; Curry, S. Structural basis of the drug-binding specificity of human serum albumin. *J. Mol. Biol.* **2005**, *353*, 38–52. [CrossRef] [PubMed]
12. Ryan, A.J.; Ghuman, J.; Zunszain, P.A.; Chung, C.-W.; Curry, S. Structural basis of binding of fluorescent, site-specific dansylated amino acids to human serum albumin. *J. Struct. Biol.* **2011**, *174*, 84–91. [CrossRef] [PubMed]
13. Trynda-Lemiesz, L.; Wiglusz, K. Interactions of human serum albumin with meloxicam: Characterization of binding site. *J. Pharm. Biomed. Anal.* **2010**, *52*, 300–304. [CrossRef] [PubMed]
14. Ascenzi, P.; Leboffe, L.; di Masi, A.; Trezza, V.; Fanali, G.; Gioia, M.; Coletta, M.; Fasano, M.; Permyakov, E.A. Ligand binding to the FA3-FA4 cleft inhibits the esterase-like activity of human serum albumin. *PLoS ONE* **2015**, *10*, e0120603. [CrossRef] [PubMed]
15. Bhattacharya, A.A.; Curry, S.; Franks, N.P. Binding of the general anesthetics propofol and halothane to human serum albumin: High resolution crystal structures. *J. Biol. Chem.* **2000**, *275*, 38731–38738. [CrossRef] [PubMed]
16. Bolattin, M.B.; Nandibewoor, S.T.; Joshi, S.D.; Dixit, S.R.; Chimatadar, S.A. Interaction between carisoprodol and bovine serum albumin and effect of β-cyclodextrin on binding: Insights from molecular docking and spectroscopic techniques. *RSC Adv.* **2016**, *6*, 63463–63471. [CrossRef]
17. Wang, S.; Wang, M.; Liu, Y.; Hu, D.; Gu, L.; Fei, X.; Zhang, J. Effect of Rapamycin Microspheres in Sjögren Syndrome Dry Eye: Preparation and Outcomes. *Ocul. Immunol. Inflamm.* **2019**, *27*, 1357–1364. [CrossRef] [PubMed]
18. Jahanban-Esfahlan, A.; Dastmalchi, S.; Davaran, S. A simple improved desolvation method for the rapid preparation of albumin nanoparticles. *Int. J. Biol. Macromol.* **2016**, *91*, 703–709. [CrossRef] [PubMed]
19. Roy, A.S.; Dinda, A.K.; Pandey, N.K.; Dasgupta, S. Effects of Urea, Metal Ions and Surfactants on the Binding of Baicalein with Bovine Serum Albumin. *J. Pharm. Anal.* **2016**, *6*, 256–267. [CrossRef] [PubMed]
20. Ksenofontov, A.A.; Bocharov, P.S.; Ksenofontova, K.V.; Antina, E.V. Water-soluble BODIPY-based fluorescent probe for BSA and HSA detection. *J. Mol. Liq.* **2021**, *345*, 117031. [CrossRef]
21. Sulkowska, A. Interaction of drugs with bovine and human serum albumin. *J. Mol. Struct.* **2002**, *616*, 227–232. [CrossRef]
22. Kandagal, P.B.; Seetharamappa, J.; Ashoka, S.; Shaikh, S.; Manjunatha, D. Study of the interaction between doxepin hydrochloride and bovine serum albumin by spectroscopic techniques. *Int. J. Biol. Macromol.* **2006**, *39*, 234–239. [CrossRef] [PubMed]
23. Datta, S.; Halder, M. Detailed scrutiny of the anion receptor pocket in subdomain IIA of serum proteins toward individual response to specific ligands: HSA-pocket resembles flexible biological slide-wrench unlike BSA. *J. Phys. Chem. B* **2014**, *118*, 6071–6085. [CrossRef] [PubMed]
24. Franco, D.P.; Pereira, T.; Vitorio, F.; Nadur, N.; Lacerda, R.; Kümmerle, A. The importance of cumarins for medicinal chemistry and the development of bioactive compounds in the last years. *Quím. Nova* **2021**, *44*, 180–197. [CrossRef]
25. Carneiro, A.; Matos, M.J.; Uriarte, E.; Santana, L. Trending topics on coumarin and its derivatives in 2020. *Molecules* **2021**, *26*, 501. [CrossRef] [PubMed]
26. Borges, F.; Roleira, F.; Milhazes, N.; Santana, L.; Uriarte, E. Simple coumarins and analogues in medicinal chemistry: Occurrence, synthesis and biological activity. *Curr. Med. Chem.* **2005**, *12*, 887–916. [CrossRef] [PubMed]
27. de Souza, A.R.; Boza, I.; Ximenes, V.; Yoguin, M.; Dávila-Rodriguez, M.-J.; Morgon, N.; Caracelli, I. Elucidação da quiralidade induzida na molécula dansilglicina na complexação com a proteína albumina do soro humano (HSA). *Quím. Nova* **2019**, *42*, 135–142. [CrossRef]
28. Liu, Y.-S.; Fang, Y.; Ramani, K. Using least median of squares for structural superposition of flexible proteins. *BMC Bioinform.* **2009**, *10*, 29. [CrossRef] [PubMed]
29. Gutierrez, J.A.; Falcone, R.D.; Silber, J.J.; Correa, N.M. Role of the medium on the C343 inter/intramolecular hydrogen bond interactions: An absorption, emission, and $^{1}$H NMR investigation of C343 in benzene/n-heptane mixtures. *J. Phys. Chem. A* **2010**, *114*, 7326–7330. [CrossRef] [PubMed]
30. Bujacz, A.; Zielinski, K.; Sekula, B. Structural studies of bovine, equine, and leporine serum albumin complexes with naproxen. *Proteins* **2014**, *82*, 2199–2208. [CrossRef] [PubMed]
31. Johnson, E.R.; Keinan, S.; Mori-Sánchez, P.; Contreras-García, J.; Cohen, A.J.; Yang, W. Revealing noncovalent interactions. *J. Am. Chem. Soc.* **2010**, *132*, 6498–6506. [CrossRef] [PubMed]

32. Kozuch, S.; Martin, J.M.L. Halogen bonds: Benchmarks and theoretical analysis. *J. Chem. Theory Comput.* **2013**, *9*, 1918–1931. [CrossRef] [PubMed]
33. Peters, T., Jr. *All About Albumin: Biochemistry, Genetics, and Medical Applications*; Academic Press: San Diego, CA, USA, 1995.
34. Jiskoot, W.; Visser, A.J.W.G.; Herron, J.N.; Sutter, M. Fluorescence Spectroscopy. In *Methods for Structural Analysis of Protein Pharmaceuticals*; AAPS Press: Arlington, TX, USA, 2005; p. 27.
35. Guizado, T.R.C. Estudos Computacionais da Interação de Porfirinas e Seus Complexos de Ferro com Albumina Sérica Humana. Master's Thesis, Pontifícia Universidade Católica do Rio de Janeiro, Rio de Janeiro, Brazil, 2008.
36. Neto, G.L.B.; Baptista, E.; Becca, G.; Nakatani, H.; Souza, V. Interações competitivas de complexos de rutênio contendo dimetilsulfóxido e ligantes N-heterocíclicos com albumina de soro humano. *Quím. Nova* **2020**, *43*, 261–270. [CrossRef]
37. Nakata, A.; Imamura, Y.; Otsuka, T.; Nakai, H. Time-dependent density functional theory calculations for core-excited states: Assessment of standard exchange-correlation functionals and development of a novel hybrid functional. *J. Chem. Phys.* **2006**, *124*, 094105. [CrossRef] [PubMed]
38. Hildebrand, J.H.; Benesi, H.A. Interaction of iodine with aromatic hydrocarbons. *Nature* **1949**, *164*, 963. [CrossRef]
39. Lakowicz, J.R. *Principles of Fluorescence Spectroscopy*, 3rd ed.; Springer: New York, NY, USA, 2006. [CrossRef]
40. Rawel, H.M.; Meidtner, K.; Kroll, J. Binding of selected phenolic compounds to proteins. *J. Agric. Food Chem.* **2005**, *53*, 4228–4235. [CrossRef] [PubMed]
41. Roy, S. Fluorescence quenching methods to study protein-nucleic acid interactions. *Methods Enzymol.* **2004**, *379*, 175–187. [CrossRef] [PubMed]
42. Zsila, F.; Hazai, E.; Sawyer, L. Binding of the pepper alkaloid piperine to bovine β-lactoglobulin: Circular dichroism spectroscopy and molecular modeling study. *J. Agric. Food Chem.* **2005**, *53*, 10179–10185. [CrossRef] [PubMed]
43. Góes Filho, L.S. Estudo do Efeito de Solventes nas Propriedades Espectroscópicas do Antibiótico Norfloxacina: Absorção, Fluorescência Estacionária e Resolvida No Tempo. Ph.D. Thesis, Pontifícia Universidade Católica do Rio de Janeiro, Rio de Janeiro, Brazil, 2010.
44. Dasgupta, A. Immunoassays and Issues with Interference in Therapeutic Drug Monitoring. In *Clinical Challenges in Therapeutic Drug Monitoring*; Dasgupta, A., Ed.; Elsevier: Amsterdam, The Netherlands, 2016; pp. 17–44. [CrossRef]
45. Huang, C.Y. Determination of binding stoichiometry by the continuous variation method: The Job plot. In *Methods in Enzymology*; Colowick, S.P., Kaplan, N.O., Eds.; Academic Press: New York, NY, USA, 1982; Volume 87, pp. 509–525. [CrossRef]
46. Olson, E.J.; Bühlmann, P. Getting more out of a Job plot: Determination of reactant to product stoichiometry in cases of displacement reactions and n:n complex formation. *J. Org. Chem.* **2011**, *76*, 8406–8412. [CrossRef] [PubMed]
47. Pitman, S.J.; Evans, A.K.; Ireland, R.T.; Lempriere, F.; McKemmish, L.K. Benchmarking basis sets for density functional theory thermochemistry calculations: Why unpolarised basis sets and the polarised 6-311G family should be avoided. *J. Phys. Chem. A* **2023**, *127*, 10834–10848. [CrossRef] [PubMed]
48. Mahamiya, V.; Bhattacharyya, P.; Shukla, A. Benchmarking Gaussian basis sets in quantum-chemical calculations of photo-absorption spectra of light atomic clusters. *ACS Omega* **2022**, *7*, 48261–48271. [CrossRef] [PubMed]
49. Autschbach, J.; Ziegler, T.; van Gisbergen, S.J.A.; Baerends, E.J. Chiroptical properties from time-dependent density functional theory. I. Circ. Dichroism Spectra Org. molecules. *J. Chem. Phys.* **2002**, *116*, 6930–6940. [CrossRef]
50. Graciani, F.S.; Ximenes, V.F. Investigation of human albumin-induced circular dichroism in dansylglycine. *PLoS ONE* **2013**, *8*, e76849. [CrossRef] [PubMed]